Available online at www.sciencedirect.com

ScienceDirect

Procedia CIRP 115 (2022) 119–124

www.elsevier.com/locate/procedia

10th CIRP Global Web Conference – Material Aspects of Manufacturing Processes

Process Monitoring of a Vibration Dampening CFRP Drill Tube in BTA deep hole drilling using Fibre-Bragg-Grating Sensors

Jannik Summa[a,*], Sebastian Michel[b], Moritz Kurkowski[c], Dirk Biermann[b], Markus Stommel[c,d], Hans-Georg Herrmann[a,e]

[a]*Fraunhofer Institute for non-destructive testing IZFP, 66123 Saarbrücken, Germany*
[b]*TU Dortmund University, Institute of Machining Technology, Baroper Str. 303, 44227 Dortmund, Germany*
[c]*Leibniz Institute of Polymer Research Dresden, Hohe Str. 6, 01069 Dresden, Germany*
[d]*Technical University Dresden, Institute of Materials Science, 01062 Dresden, Germany*
[e]*Saarland University, Chair for Leightweight Systems, Campus E3.1, 66123 Saarbrücken, Germany*

* Corresponding author. Tel.: +49 681-9302-3933; *E-mail address:* jannik.summa@izfp.fraunhofer.de

Abstract

The large tool length in BTA deep hole drilling often leads to strong torsional vibrations of the tool system, leading to a reduced bore hole quality failures. When substituting steel drill tubes with tubes from composite material, the laminate structure dampens these vibrations. Secondly, the integration of sensors allow to monitor process vibrations. This contribution introduces a new sensor platform to measure process vibrations, feed force and drilling torque using Fibre-Bragg Grating Sensors. The presented experimental results focus on characteristic frequency spectra with natural torsional and compression frequencies of the CFRP drill tube, which show variations due to changed feed.

Keywords: Deep hole drilling; CFRP drill tube; Process Monitoring; Fibre-Bragg-Grating Sensors

1. Introduction

Producing high-quality bore holes with large drilling depths is a major challenge in machining and therefore requires special drilling methods and tools [1,2]. BTA (Boring & Trepanning Association) deep hole drilling is typically used for bore holes with high length-to-diameter ratios in the diameter range from 12 mm to 500 mm [3]. Exemplary industrial applications are the manufacturing of hydraulic cylinders or the machining of drilling equipment for the oil and gas exploration industry. The tool system in BTA deep hole drilling consists of a drill tube and a drill head. The cutting edges at the drill head are arranged asymetrically. The resulting radial forces are transmitted to the bore hole wall via guide pads on the circumference of the drill head, resulting in high surface qualities due to a smoothing of the feed marks of the cutting edges [4]. However, due to the length of the tool system, the process dynamics have a significant effect on the machining result [5–7]. The cutting engagement and the contact of the guide pads with the bore hole surface often lead to torsional vibrations and an oscillation of the drill tube in circumferential direction [5]. Regardless of the cutting parameters the stick-slip effect created by the friction between the guide pads and the bore hole wall promotes the generation of self-excited vibrations, which occur typically in one of the natural frequencies or a superposition of the natural frequencies of the tool system [5,8,9].

10.1016/j.procir.2022.10.060

1.1. CFRP drill tube for dampening

Since the influence of external damping systems is limited on the free drill tube length inside the bore hole, vibrations in deep hole drilling can only be dampened via the drill tube, e.g. by material damping. Nagano and Lee were able to demonstrate the positive effect of carbon fibre-reinforced plastics (CFRP) on process vibrations in drilling experiments [10,11]. The dampening properties of fibre-reinforced plastics result from the inhomogeneous structure consisting of stiff fibres and a dampening polymeric matrix. In previous work, it was shown that torsional vibrations could be significantly reduced in deep hole drilling by using a composite drill tube. Experimental results showing the dampening effect of the CFRP drill tube compared to a conventional steel drill tube are reported in [12,13].

1.2. Process Monitoring using embedded sensors

Vibration measurement is a very important tool in modern engineering systems, e.g. civil infrastructure, mechanical engineering systems and more. Since abnormal behavior or damaged materials can cause vibrations, sensing technologies play an important role for monitoring to avoid premature failures [14]. Fibre optical sensors are reported to find increasing attention for structural-health monitoring (SHM) applications. Fibre-Bragg-Grating (FBG) based sensors are typically found in the aerospace industry, e.g. for the detection of skin-spar failure [15], shape and strain sensing of large-scale structural winglets, measuring residual strain during and after manufacturing [16] or as part of complex vibrational transducers [14,17]. FBGs have the advantages of small size, heat and corrosion resistance and being light weight, non-conductive and immune to electromagnetic interference, while allowing to measure very large strains with good long term stability and sensor multiplexing [17,18]. Furthermore, FBGs are suitable for the direct embedment in composite structures [18] and distributed sensing without unwanted fibre bend loss, which makes them the uppermost candidates for vibration measurement [14].
However, a major drawback of FBG sensors are the egress and ingress points, since the measurement fibres are vulnerable to damage even when handled carefully [18]. As a second disadvantage the literature discusses, whether embedment of FBG deteriorates the mechanical performance of composites [16]. Variations of young's modulus and tensile strength, e.g. caused by bridging [19], depends on the location and orientation of the integrated sensor fibre with respect to the reinforcing-fibres.
In principle, the FBGs functionality is based on the grating, which is engraved at each measuring point. Dependent on the grid spacing Λ, the Bragg-Grating reflects the emitted light within a certain wavelength range [14,20]. If the optical fibre, or the grating respectively, undergoes deformation due to stretching or temperature, the center wavelength of the reflected light λ_B will change adequately. It follows from [14]:

$$\frac{\Delta\lambda_B}{\lambda_B} = (1 - p_e)\Delta\varepsilon + (\alpha + \theta)\Delta T \qquad (1)$$

In the equation p_e represents the elasto-optical coefficient of the fibre, $\Delta\varepsilon$ the longitudinal strain variation, ΔT the temperature change, θ the thermo-optic coefficient and α the coefficient of the thermal expansion of the fibre. Thus, the FBG-signal comprises of mechanical strain and temperature changes, which can be separated in the analysis of the measurement data. Schukar et al. [21] suggest a self-compensating method with superstructured FBGs, instead of additional temperature measurements. Yi et al. [22] arranged three FBGs oriented 120° with respect to each other to separate bending and torsion.
However, connecting the sensors for data acquisition on a fast rotating systems is still a challenge. Therefore, this contribution addresses the deployment of a sensor platform for multimodal sensing and data transition during operation. Hereby, the disturbing influences due to high radial forces on the optics are questionable. In addition, FBG sensors, unlike strain gages, are difficult to compensate for transverse dependencies. Therefore, the paper additionally deals with the validation of the FBG signals.

2. Design and simulation of the CFRP drill tube

The design of the wound FRP drill tube is carried out using finite element analysis (FEA). A detailed description can be found in [13]. For this purpose, the values of laminate stiffness and strength are determined experimentally for three fibre types and an epoxy resin matrix. The characteristic values for tension, compression and shear are determined in accordance with international standards using wound specimens cured in a flat geometry [23,24]. The geometry of the drill tube (d_i = 40 mm, d_a = 51 mm, l = 2650 mm) is defined by the requirements of the deep hole drilling process and the nominal bore hole diameter of d = 60 mm. Within the FEA a feed force of F_f = 20 kN and a drilling torque of M_B = 1000 Nm is assumed, while the fibre angle and fibre types are varied. The simulative design aims at a laminate with high torsional and high axial stiffness to withstand the feed forces as well as the drilling torque. In addition, the natural frequencies are investigated simulatively. Based on the simulation results, a FRP drill tube with a laminate structure of $[\pm 6_2^{CF}/\pm 45_2^{GF}/\pm 45_2^{CF}]$ is manufactured. Table 1 shows the fibre and matrix materials used in the fibre winding process. Finally, a two-component epoxy adhesive is used to join the drill tube with metallic adapters to connect the drill head and to clamp the tube in the tool spindle of the deep hole drilling machine.

Table 1. Material for laminate construction

Material type and abbreviation	Material	Fibre volume content
Carbonfibre (CF)	STS40 F13, 24K, 1600tex (Toho Tenax)	0,55
Glasfibre (GF)	SE1200, 2400tex (Owens Corning)	0,62
Matrix	Epikote MGS RIMR935, Epikure MGS RIMH 937 (Hexion Inc.)	-

3. Sensor platform for deep hole drilling

In order to enable an in-process measurement during the deep hole drilling process with FBG sensors a rotating sensor plattform is integrated at the tool spindle of the deep hole drilling machine (see Fig. 1.). The main components mounted on the platform are the interrogator for demodulation of the FBG signals and two multichannel digital measuring amplifier. This al-

lows multimodal sensing based on different physical principles. However, the important quantities are drilling torque, feed force, vibration and temperature of the drill tube as well as rotation speed and radial acceleration which can affect the electronic devices.

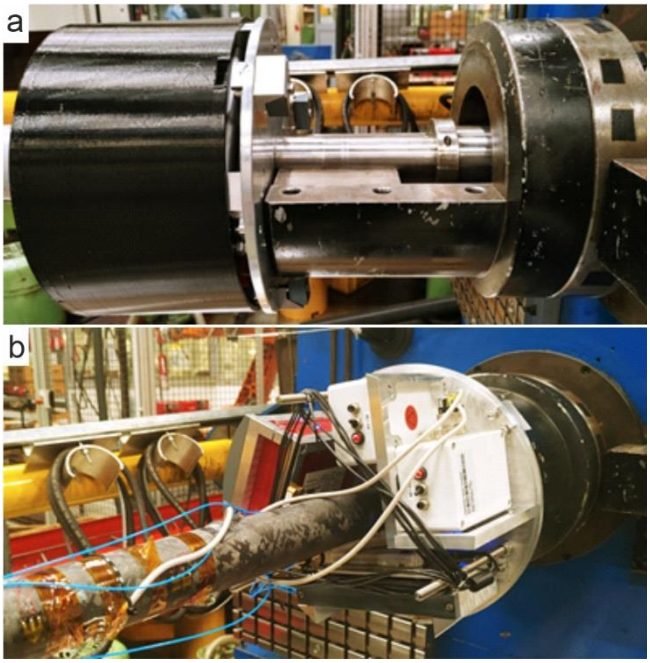

Fig. 1. (a) mounting the platform and the drill tube on the drill chuck, (b) platform with interrogator (red) and two measuring amplifiers (white)

The used interrogator is a SwitchedGator (Photonfirst, formerly tft-fos). It has 8 optical channels, a sampling speed of 19.23 kHz, a wavelength range of 1515-1585 nm, a wavelength repeatability of 1 pm, a dynamic range of 4.8 nm and the FBG/ full width half maximum range of 150-400 pm. For integrational purposes its small dimension and weight (540 g) are important advantages. Both of the digital measuring amplifiers are GSV-4BT M12 (ME-Systeme). Each possesses 4 channels, which can be used for strain gauges (quarter-, half or full bridge), PT1000 thermo-sensors, for 5 V input and for potentiometric sensors (acceleration sensor). It also works in the measuring range of 2 mV/V or 10 mV/V.

The core of the station is a single board computer (Latte Panda Delta), which controls the measuring devices. The Labview-based software enables to configure the measuring parameters of each device before saving the parameters, operator name, date and time as metadata. Proceeding to the measurement mode, the system collects the acquired data from the devices and sends it to an external device per TCP-IP connection. To avoid delays due to overload of the single board computer, data processing and inline-analysis of the measured data is performed on the external device. In the current version, a local WIFI connection is built between the single board computer and an external PC. For the TCP IP connection, the single board computer works as the server, the external PC as the client. In principle, the single board computer can also be connected to a server or the machine control.

The platform is fixed on the drill chuck with three M12 screws allowing the measuring devices to rotate synchronous to the drill tube. Customized holders on the platform ensure the fixation of the equipment against radial acceleration. However, a one-dimensional accelerometer detects the g-forces acting on the electronic devices. Additional cable holders can counteract movements of cables and fibres and simplify the handling. Finally, the platform holds a powerful battery for power supply of the interrogator and the single board computer, while the GSV-4BTs have their own integrated batteries.

4. Sensor application and experimental setup

For the characterisation of the dynamic tool behaviour, three FBG arrays are applied to the surface of the CFRP drill tube using a two component reactive epoxy adhesive. Each of the arrays has a side lobe suppression of greater than -15 dB, a lead in of 500 mm with a Hytrel buffer and a FC/APC connector, which is a standard configuration. The characteristic centre wavelengths, fibre placement and orientations as well as the values for full width half maximum (FWHM) are summarized in Table 2. Based on the arrangement of strain gauges in a full bridge, 0°/90° orientation is intended for axial strain and ±45° for torsional strain measurements, the arrangement of array Nº 2 aims to compensate the bending influences [22]. Special attention should be drawn to the fact that only the array with three FBGs (array Nº 2) was read out in the presented experiments. Hence, the FBG array is read continuously without reading timeout and without switching to other channels.

In addition, strain gauges with a nominal resistance of 350 Ohm and a measuring grid width of 6 mm are applied to the drill tube surface. Since feed force and the drilling torque are to be measured, a bridge circuit compensates the influence of bending of the drill tube on the measurement results. To measure the feed force, two 0°/90° T-rosette strain gages are applied at a distance of 180° from each other. Accordingly, two ±45° T-rosettes are applied at a distance of 90° from each other to measure the drilling torque.

Table 2. Parameters of the applied FBG sensor arrays

FBG array Nº	Nº of FBGs on array	Center WL [nm]	FWHM [nm]	Orientation	Relative Position
1	2	1544.946	0.262	0°	Adjacent to each other
		1567.946	0.250	90°	
2	3	1526.934	0.278	60°	120° to each other
		1544.910	0.270	60°	
		1562.863	0.247	60°	
3	4	1536.011	0.190	-45°	2 pairs with Distance of 180°
		1545.018	0.183	+45°	
		1553.983	0.196	+45°	
		1562.965	0.196	-45°	

The drilling tests with the CFRP drill tube are carried out on a Giana GGB560 BTA deep hole drilling machine with workpieces consisting of 42CrMo4+QT. Without an additional dampening system the characteristic dynamic behavior with high torsional vibrations already occurs at very low drilling depths. Fig. 2. depicts the experimental setup with the CFRP drill tube and the mounted sensor platform.

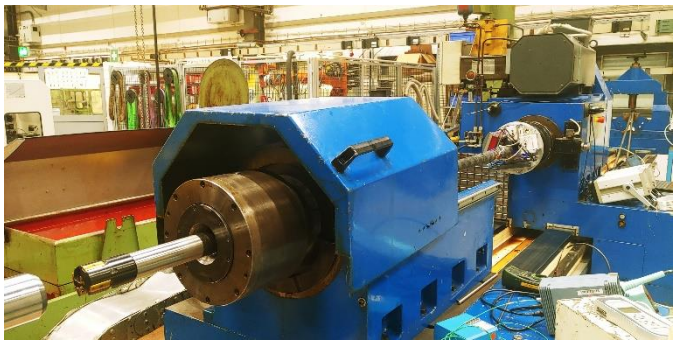

Fig. 2. Giana GGB560 BTA deep hole drilling machine (blue) with mounted CFRP drill tube, drill head (left) and the sensor platform

Before the actual drilling experiments, a calibration is needed to convert the measuring signals into the desired values of feed force and drilling torque. For this purpose, an axial force of 1, 2 and 3 kN respectively as well as a torque of 50, 75 and 100 Nm were manually applied to the end of the CFRP tube while measuring the sensor response. The tube was fixed in the spindle and supported in the drilling bush at the other end to avoid bending of the tube. Table 3 summarizes the determined conversion factors and the corresponding errors.

Table 3. Conversion factors from strain gauge sensors and FBG sensors on array N° 2 to feed force and drilling torque

	Feed Force [kN]		Drilling Torque [Nm]	
DMS 0°/90° mV/V	$7.63\ 10^{-3}$	$\pm 1.00\ 10^{-4}$	$-1{,}20\ 10^{-4}$	$\pm 9.75\ 10^{-7}$
DMS ±45° mV/V	$5.73\ 10^{-4}$	$\pm 4.00\ 10^{-5}$	$3.87\ 10^{-3}$	$\pm 3.42\ 10^{-5}$
FBG 1 µm/mm	$5.83\ 10^{-3}$	$\pm 1.99\ 10^{-4}$	$1.34\ 10^{-3}$	$\pm 1.51\ 10^{-5}$
FBG 2 µm/mm	$-1.83\ 10^{-3}$	$\pm 6.04\ 10^{-5}$	$1.28\ 10^{-3}$	$\pm 1.11\ 10^{-4}$
FBG 3 µm/mm	$5.65\ 10^{-3}$	$\pm 7.0910^{-5}$	$1.24\ 10^{-3}$	$\pm 2.39\ 10^{-5}$

5. Experimental results

For a drilling depth of l_t = 120 mm and a volume flow of the deep hole drilling oil of 275 l/min, experimental results of three different process parameter sets are compared in the following. The cutting velocity is kept constant at v_c = 60 m/min, whereas the feed varies from f = 0.15 mm to f = 0.225 mm and f = 0.3 mm.

The measured data is given in Fig. 3. showing the drilling torque measured with FBG 1 and the strain gauge signal, the feed force measured by strain gauges as well as the time-frequency analysis of the torsional vibrations. For the latter, the (FBG measured) drilling torque is devided into 1 s intervals and processed with a FFT algorithm. It should be stated that a compensation procedure is applied to the measurement data to display the correct values of drilling torque and feed force. First, the FBG-sensor data is temperature compensated. This is realised using the sensor data from FBG 3 to determine the change in temperature during the process. Secondly, the displayed feed force already takes into account that the drilling torque leads to a negative display of the feed force for the strain gauge 'DMS' with 0°/ 90° orientation (see the negative conversion factor in Table 3). From the drilling torque signal the start of the process is evident. Subsequently, the torque and the feed force built up, as the drill head engages with the workpiece. This is clearly visible in the FBG and the strain gauge signal. Over the whole process, both signals show a similar course with respect to time. Though, the FBG signal indicates a higher mean value and higher vibration amplitude of the drilling torque, which may be due to a non-compensated contribution of the feed force. To estimate the possible error of the FBG signal, note that a feed force of F_f = 7 kN would falsely indicate a drilling torque of approximately M_B = 30 Nm. Ultimately, it can be concluded from the comparison with the strain gauge signal (Fig. 3. (a)) that the FBG signal is valid for the characterization of the dynamic behaviour of the process.

Comparing the FBG signals of the three experiments shows that the base level of drilling torque increases from a feed of f = 0.15 mm over f = 0.225 mm to f = 0.3 mm. In comparison, the vibration amplitude does not increase proportionally to the applied feed. The amplitude of the drilling torque increases from approximately M_B = 115 Nm for f = 0.15 mm to M_B = 121 Nm for f = 0.225 mm and M_B = 122 Nm f = 0.3 mm. These values prove the strong dampening effect compared to a steel drill tube. In [13] the measured vibration amplitude of drilling torque for a steel drill tube with vc = 60 m/min and f = 0.225 mm amounted to 389 Nm. However, at the end of the experiment with a feed of f = 0.3 mm (Fig. 3. (a), right) the amplitude rises sligthly. The course of all three tests shows a short vibration maximum shortly after reaching the working regime representing the initial contact of the guide pads of the drill head with the workpiece.

Analysis of the feed force (Fig. 3. (b)) signal shows a monotonic drift from the beginning to the end of the process. Since the full bridge compensates for the temperature-dependent resistance of the strain gauges, this is probably due to the direction-dependent temperature expansion of the CFRP. However, since there is no monotic behavior in the offset values (Offset at process end: f = 0.15 mm: 0.81 kN, f = 0.225 mm: 1.26 kN, f = 0.3 mm: 0.79 kN), the authors assume no systematic dependency behind the drift and process time or process parameters. Comparing the feed forces of the three process parameter sets, the base level clearly increases according to the applied feed from f = 0.15 mm over f = 0.225 mm to f = 0.3 mm. The vibration is of comparable magnitude in all three experiments, wherein the maximum at 10 mm drilling depth is only of noticeable magnitude for the experiments with f = 0.225 mm and f = 0.3 mm.

Additionally, Fig. 3. (c) displays the FFT-results of the drilling torque of the three experiments. Plotting the vibration amplitude with respect to frequency and drilling depth reveals characteristic line-spectra. First, it should be noted that occasionally the overdrive of the FBG signals is evident, leading to a blurry spectrum. Since this occurs more frequently with higher feed, the authors assume that high accelerations as well as a thick adhesive layer have a negative effect on the signal-quality for the surface-applied FBG sensors. However, in the range of the process before the drill head engages with the working piece, denoted in Fig. 3. (c) as negative drilling depth, the free rotation of the drill tube results in a vibration frequency of 214 Hz. As the drilling process starts, it shifts to lower frequencies. Depending on the feed force it reaches 203 Hz (f = 0.15 mm) or 198 Hz (f = 0.225 mm, f = 0.3 mm) respectively. The degree of frequency shift is consistent with the measured feed force. The greater the feed force, the greater the downward shift of the natural frequency.

Besides the first natural torsional frequency (214 Hz), the spectrum gives additional characteristic lines. Due to comparison with FEA, the equidistant lines at 400 Hz, 600 Hz and 800 Hz

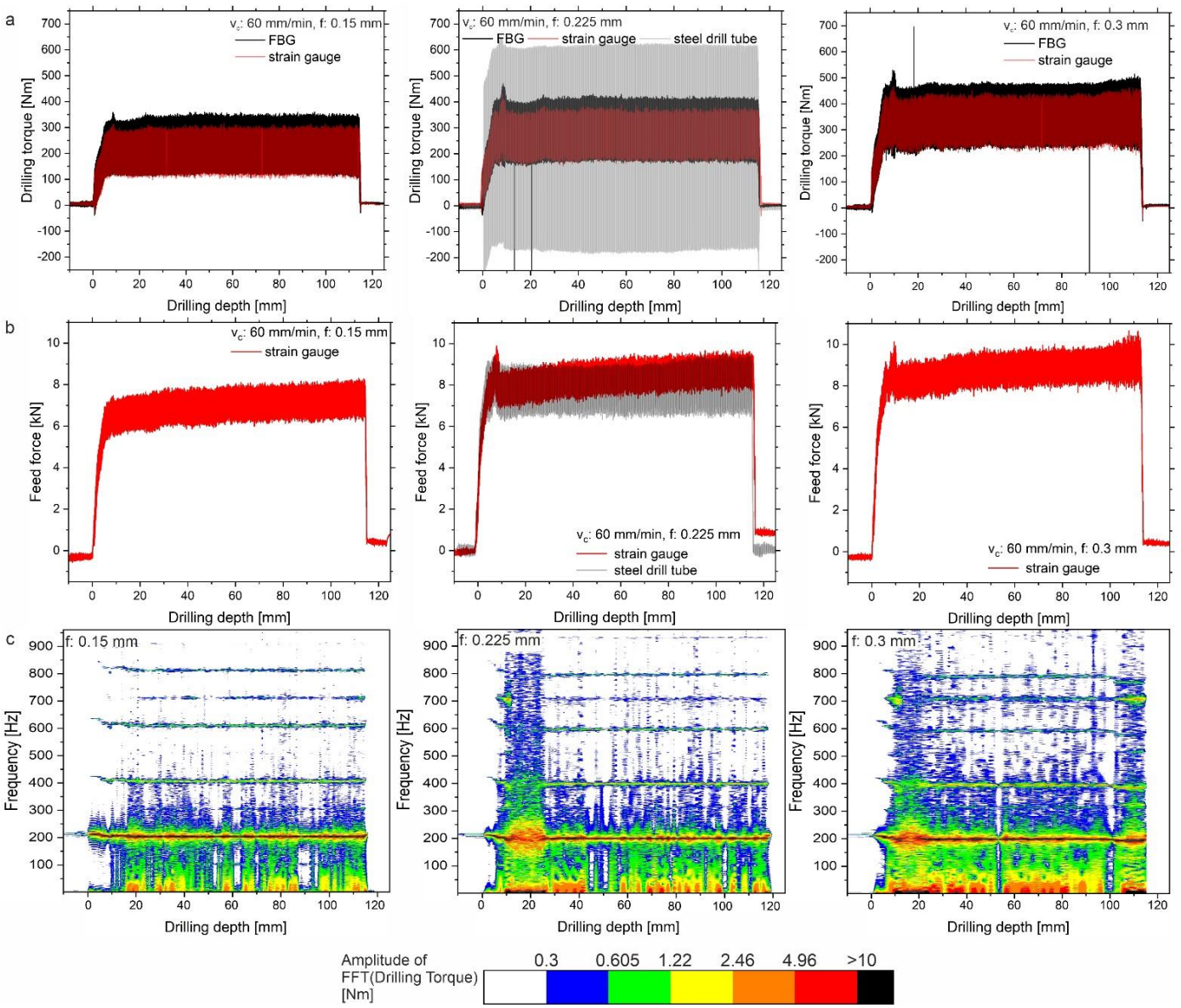

Fig. 3. (a) comparison of drilling torque for FBG 1 on the CFRP drill tube (black line), strain gauges on CFRP drill tube (red line) and for strain gauges on the steel drill tube (grey line), (b) feed force measured with strain gauges and (c) FFT-analysis of the FBG-signal from (a) as a colour-plot of the drilling torque amplitude as a function of the frequency and drilling depth, the colour bar gives the amplitude

are identified as harmonics of the first torsional natural frequency.

Further, it is evident that the frequencies of these characteristic lines change in the beginning of the process and remain constant during a stable state. In the early process stage, the shift of the frequencies accompanies strong noising of the signal and broadening of the first torsional natural frequency. Regardless of the feed, this effect starts after a drilling depth of approximately 5 mm and vanishes after approximately 25 mm. These effects can be assigned to the drill head. The 5 mm correspond to the distance between the cutting edge and the guide pads. Subsequently, the guide pads leave the drill bush and engage with the workpiece over the following distance of 20 mm. This effect agrees with the reported promotion of self-excited vibrations [5,8,9]. Changes of the process conditions may lead to changes in the spectrum, as seen for a feed of f = 0.3 mm after l_t = 100 mm drilling depth (Fig. 3. (c), right). However, additional lines with low intensity lie at 310 Hz and approximately 705 Hz. In the area of the increased vibration amplitude of the test with a feed of 0.3 mm, the vibrations start at 100 mm with approximately 520 Hz. Again, FEA helps to identify 310 Hz as well as 705 Hz as two modes of compression natural frequencies of the CFRP drill tube. It is worth mentioning that the compression modes do not change in frequency but remain constant. Secondly, a peak of the 705 Hz frequency can be noticed in the experiments with a feed of 0.225 mm and 0.3 mm, between 5 and 15 mm drilling depth. This peak fits perfectly to the maximum in the feed force diagrams at approximately 10 mm drilling depth. A possible explanation is that the guide pads initial engagement with the workpiece. Hence, the higher friction causes increased feed force and drilling torque and ultimately a higher vibration in the compression mode. For the final analysis, the local maxima of the FFT vibration amplitude (Fig. 3. (c)) exceeding 2 Nm in magnitude are plotted against the frequency (see Fig. 4.). The plot clearly points out a shift of the line spectra to lower frequencies from a feed of f = 0.15 mm (black dots) over f = 0.225 mm (red dots) to f = 0.3 mm (blue dots). In particular, the centers of gravity of the point cloud shift. In addition, for the experiment at a feed of f = 0.225 mm

local maxima at a frequency of 600 Hz occur more frequently. The same can be seen for a feed of f = 0.3 mm at 700 Hz. This feed-dependent shift of the vibration frequencies and the occurrence of certain resonant frequencies, e.g. at 600 Hz and 700 Hz, suggests a very good classification of the process vibrations, e.g. using linear discriminant analysis.

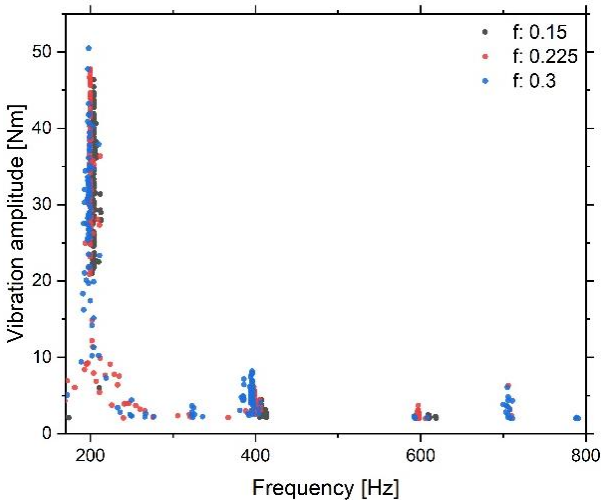

Fig. 4. scatter plot of vibration amplitude over frequency containing the local maximum values of each of the three experiments

6. Conclusion

This contribution showed a newly developed sensor platform for process monitoring of drilling torque, feed force and vibrations with FBG sensors applied to a CFRP drill tube for BTA deep hole drilling. The advantages of the sensor platform are the integrated power supply and the wireless data transfer. The measuring devices rotate with the drilling tube and the connected sensors while the acquired data is send to a client or external device via TCP IP connection.

For process monitoring, several FBG sensors were applied. After compensation of the temperature influence, the drilling torque determined by the FBG sensors could be validated by conventional strain gauges.

Based on the obtained data with the FBGs and the sensor platform the process vibrations were characterised. Feed force, drilling torque and torsional vibrations demonstrate the damping effect compared to a steel drill tube. From the time-frequency spectra and from a FEA of the CFRP drill tube it is evident that the tube vibrates in torsion and compression natural frequencies. In addition, the vibration spectra show a characteristic shift of the torsional natural frequencies, whereas the compression natural frequencies at 310 and 705 Hz remain constant. Additionally, process influences from the drill head were noticeable in the line spectra, since the blurring in the range from 5 mm to approximately 25 mm agrees well with the dimensions of cutting edge and guide pads.

From these observations, characteristic features, i.e. the local maxima of the line spectra, could be derived. This finding provides the basis for further measurements with a CFRP drill tube with FBG sensors integrated in the laminate structure. The determined characteristic vibration lines and features respectively provide promising results, which allow for a classification of the process vibrations and an automated detection of a normal vibration range or an overload for the drilling process. In addition to continuous process monitoring and quality control in BTA deep hole drilling, the FBG sensor system will enable the identification of critical process conditions and a condition monitoring of the CFRP drill tube in the future.

Acknowledgements

The authors kindly thank the German Research Foundation (DFG, Project number 426328330) and the Fraunhofer Gesellschaft for the kind project funding. The authors also thank the project partners BGTB GmbH, carbovation gmbh and Kaiser Maschinenbau und Zerspanungstechnik GmbH & Co. KG.

References

[1] VDI, VDI-Richtlinie 3210, Blatt 1:Tiefbohrverfahren, Berlin, 2006.
[2] D. Biermann, F. Bleicher, U. Heisel, F. Klocke, H.-C. Möhring, A. Shih, CIRP Annals 67 (2018) 673–694.
[3] VDI, VDI-Richtlinie 3209: Tiefbohren mit äußerer Zuführung des Kühlschmierstoffes (BTA- und ähnliche Verfahren), Berlin, 1999.
[4] H. Fuß, Aspekte zur Beeinflussung der Qualität von BTA-Tiefbohrungen. Dissertation, Dortmund, 1986.
[5] O. Webber, Untersuchungen zur bohrtiefenabhängigen Prozessdynamik beim BTA-Tiefbohren. Dissertation, Dortmund, 2007.
[6] A. STEININGER, F. BLEICHER, Journal of Machine Engineering 18 (2018) 47–59.
[7] R. Stockert, Dralleffekte beim Tiefbohren, VDI-Berichte 73–80.
[8] K. Bergmann, Reibung von Führungsleisten beim Tiefbohren, tz für Metallbearbeitung 26–29.
[9] T.P. Thai, Beitrag zur Untersuchung der selbsterregten Schwingungen von Tiefbohrwerkzeugen. Dissertation, Dortmund, 1983.
[10] D.G. Lee, H. Yun Hwang, J. Kook Kim, Composite Structures 60 (2003) 115–124.
[11] S. Nagano, T. Koizumi, T. Fujii, N. Tsujiuchi, H. Ueda, K. Steel, Composite Structures 38 (1997) 531–539.
[12] Kurkowski, M., Michel, S., & Summa, J. (2021). 1, CU Reports: Internationales Mitgliedermagazin des Composites United / von/by Glocker, Anna-Lea [Ed.]. - Composites United e.V. (CU). - Augsburg: Composites United e.V. (CU). - 2699-4534 (ISSN). - 2021 (2021) 1.
[13] S. Michel, D. Biermann, M. Kurkowski, A. Spickenheuer, M. Stommel, J. Summa, H.-G. Herrmann, wt 111 (2021) 846–850.
[14] T. Li, J. Guo, Y. Tan, Z. Zhou, IEEE Sensors J. 20 (2020) 12074–12087.
[15] M. Ciminello, A. de Fenza, I. Dimino, R. Pecora, Archive of Mechanical Engineering 64 (2017) 287–300.
[16] E. Oromiehie, B.G. Prusty, G. Rajan, P. Compston, in: 2016 IEEE Sensors Applications Symposium (SAS), IEEE, 2016, pp. 1–5.
[17] Beukema Ronald P., Beukema Ronald P.
[18] M. Nicolas, R. Sullivan, W. Richards, Aerospace 3 (2016) 18.
[19] R. Liu, D. Liang, Materials & Design 31 (2010) 994–998.
[20] R. Di Sante, Sensors (Basel, Switzerland) 15 (2015)
[21] V. Schukar, E. Baitinger, F. Mewis, N. Kusche, Trennung von Dehnung und Temp, 2014.
[22] X. Yi, X. Chen, H. Fan, F. Shi, X. Cheng, J. Qian, Optics express 28 (2020) 9367–9383.
[23] DIN EN ISO 14129:1998-02, Faserverstärkte Kunststoffe_- Zugversuch an 45°-Laminaten zur Bestimmung der Schubspannungs/Schubverformungs-Kurve des Schubmoduls in der Lagenebene (ISO_14129:1997); Deutsche Fassung EN_ISO_14129:1997, Berlin, Beuth Verlag GmbH, 10.31030/7433963.
[24] DIN EN ISO 527-5:2010-01, Kunststoffe_- Bestimmung der Zugeigenschaften_- Teil_5: Prüfbedingungen für unidirektional faserverstärkte Kunststoffverbundwerkstoffe (ISO_527-5:2009); Deutsche Fassung EN_ISO_527-5:2009, Berlin, Beuth Verlag GmbH, 10.31030/1560314